J Biosci (2019) 44:88
DOI: 10.1007/s12038-019-9908-0

Protein profiling of SH-SY5Y neuroblastoma cells: The effect of rhein

Zuzana Cockova[1], Hana Ujcikova[1,2], Petr Telensky[1,3] and Jiri Novotny[1]*

[1]*Department of Physiology, Faculty of Science, Charles University, Prague, Czech Republic*

[2]*Department of Biomathematics, Institute of Physiology of the Czech Academy of Sciences, Prague, Czech Republic*

[3]*International Clinical Research Center, St. Anne's University Hospital Brno, Brno, Czech Republic*

**Corresponding author (Email, jiri.novotny@natur.cuni.cz)*

MS received 10 October 2018; accepted 8 May 2019; published online 5 August 2019

4,5-Dihydroxyanthraquinone-2-carboxylic acid (Rhein) has been shown to have various physiological and pharmacological properties including anticancer activity and modulatory effects on bioenergetics. In this study, we explored the impact of rhein on protein profiling of undifferentiated (UC) and differentiated (DC) SH-SY5Y cells. Besides that, the cellular morphology and expression of differentiation markers were investigated to determine the effect of rhein on retinoic acid-induced neuronal cell differentiation. Using two-dimensional gel electrophoresis and matrix-assisted laser desorption/ionization-time-of-flight mass spectrometry we evaluated the changes in the proteome of both UC and DC SH-SY5Y cells after 24 h treatment with rhein. Validation of selected differentially expressed proteins and the assessment of neuronal differentiation markers were performed by western blotting. Proteomic analysis revealed significant changes in the abundance of 15 proteins linked to specific cellular processes such as cytoskeleton structure and regulation, mitochondrial function, energy metabolism, protein synthesis and neuronal plasticity. We also observed that the addition of rhein to the cultured cells during differentiation resulted in a significantly reduced neurite outgrowth and decreased expression of neuronal markers. These results indicate that rhein may strongly interfere with the differentiation process of SH-SY5Y neuroblastoma cells and is capable of inducing marked proteomic changes in these cells.

Keywords. Neuronal differentiation; proteomics; rhein; SH-SY5Y cells

Abbreviations: GAP43, growth-associated protein 43; MAP2, microtubule-associated protein 2; NSE, neuron-specific enolase; PCNA, proliferating cell nuclear antigen; PRX, peroxiredoxin; RA, retinoic acid; SNP, synaptophysin; TH, tyrosine hydroxylase

1. Introduction

The human neuroblastoma cell line SH-SY5Y is a result of a three-time cloned parental SK-N-SH cell line, which was originally derived from a metastatic bone tumor (Biedler *et al.* 1973; Ross *et al.* 1983). In their undifferentiated state these cells are considered to resemble immature catecholaminergic neuroblasts, characterized by markers indicative of proliferation such as proliferating cell nuclear antigen (PCNA) (Cuende *et al.* 2008) and by neuronal progenitor cell markers such as nestin (Lopes *et al.* 2010). When exposed to appropriate growth conditions, SH-SY5Y cells can be differentiated towards a phenotype reminiscent of primary neurons and express a number of mature neuronal markers, including βIII-tubulin, growth associated protein 43 (GAP43), microtubule-associated protein 2 (MAP2), synaptophysin (SNP), neuronal nuclear antigen (NeuN), synaptic associated protein 97 (SAP 97) or neuron-specific enolase (NSE) (Encinas *et al.* 2000; Cheung *et al.* 2009; Lopes *et al.* 2010). There are various protocols available for the differentiation of SH-SY5Y cells. Among the most widely accepted are the differentiation protocols that involve the application of retinoic acid (RA), sometimes in combination with a low concentration of serum (Lasorella *et al.* 1995; Yu *et al.* 2003). Exposure of SH-SY5Y cells to RA has been repeatedly shown to induce changes characteristic of mature catecholaminergic neurons with the increased expression of relevant enzymes or transporters (Khwanraj

Electronic supplementary material: The online version of this article (https://doi.org/10.1007/s12038-019-9908-0) contains supplementary material, which is available to authorized users.

et al. 2015; Lim *et al.* 2015), but an inclination towards cholinergic nature was also described (Hashemi *et al.* 2003). Such controversial findings render the neurotransmitter phenotype of SH-SY5Y cells differentiated with RA phenotype rather unclear. Nevertheless, both undifferentiated (UC) and differentiated (DC) SH-SY5Y cells have been widely used as a model to study neuronal differentiation and metabolism, neuroblastoma tumorigenesis or various aspects of neurodegenerative and neuroadaptive processes (Presgraves *et al.* 2004; Ojala *et al.* 2008; Lopes *et al.* 2010; Xie *et al.* 2010).

Rhein (4,5-dihydroxyanthraquinone-2-carboxylic acid), an important bioactive compound of a traditional Chinese medicinal herb rhubarb (Rheum officinale), exerts a variety of pharmacological effects. Experimental studies revealed that rhein possesses anti-inflammatory, anti-bacterial and anticancer properties (Zhou *et al.* 2015). Treatment with rhein induced cell cycle arrest and apoptosis in various cancer cells (Lai *et al.* 2009; Chang *et al.* 2012; Bounda *et al.* 2015). Several studies demonstrated the influence of rhein on cell differentiation. Glioma cells treated with rhein underwent a substantial morphological change, acquiring a phenotype analogous to that of matured astrocytes (Tang *et al.* 2017). Rhein was found to inhibit the differentiation of 3T3-L1 preadipocytes (Liu *et al.* 2011). Moreover, some data indicate that rhein might be suitable as a candidate drug for preventive therapy of metabolic disorders (Zheng *et al.* 2008; Sheng *et al.* 2011; Zhang *et al.* 2012). This is particularly interesting because rhein has recently been shown to inhibit some members of 2-oxoglutarate-dependent dioxygenases, including RNA m6A demethylase fat mass and obesity-associated protein (FTO), a master regulator of obesity (Chen *et al.* 2012; Li *et al.* 2016).

To date no one has attempted to investigate the impact of rhein on protein profiling of neuronal cells. This study is set out to analyze the effect of rhein on protein expression in both UC and DC SH-SY5Y neuroblastoma cells. In addition, since rhein was shown to induce differentiation in glioblastoma cells and to prevent such process in adipocytes, we sought to find out if this compound may interfere with the differentiation process of neuroblastoma cells. We have observed that rhein impeded RA-induced differentiation of SH-SY5Y cells and that 24 h treatment with rhein induced profound changes in the cellular proteome.

2. Materials and methods

2.1 *Cell culture and neuronal differentiation*

The human neuroblastoma SH-SY5Y cell line was purchased from the American Tissue Culture Collection (ATCC, CRL-2266). Cells were grown in Dulbecco's modified Eagle's medium (DMEM, #D6429, Sigma-Aldrich) containing high glucose (4500 mg/L), L-glutamine (4 mM) and sodium pyruvate (1 mM). This medium was supplemented with 10% (v/v) heat-inactivated fetal bovine serum (FBS, #10270, Gibco) and 1% antibiotic antimycotic solution (#A5955, Sigma-Aldrich). The cells were maintained at 37°C with 5% CO_2 at saturated humidity and routinely passaged (1:4) twice weekly. During periods of experimental treatments, the cells were cultured in low-serum media (1% FBS) as a means of withdrawing growth factors. Neuronal differentiation was induced in cells at 50% confluence by 10 μM all-*trans* RA (#R2625, Sigma-Aldrich) dissolved in dimethyl sulfoxide (DMSO). Differentiation proceeded for 6 days, during which the spent medium was replaced with fresh DMEM containing RA every other day. All experiments with retinoids were conducted in subdued light, and the tubes containing RA were wrapped in aluminum foil. The progress of neuronal differentiation was monitored microscopically via morphological assessment of neurite outgrowth. After 6 day cultivation in the presence of RA, SH-SY5Y cells exhibited a typical neuronal morphology, ranging from simple bipolar to large, extensively branched, multipolar cells. For studying the effect of rhein, this compound was dissolved in 0.1 M NaOH to make a 10 mM stock solution. Rhein was added to the culture media at 10 μM concentration. Cells were incubated in the presence of rhein for 24 h.

2.2 *Neurite outgrowth analysis*

SH-SY5Y cells were seeded in six-well plates and grown for 6 days in the absence or presence of RA. The cellular morphology was periodically observed under an inverted microscope (Arsenal AIF 5013i-T, 10× eyepieces and 20× objective lens) and photographed by using a CCD digital camera (Tucsen TCC-5.0ICE). To determine the neurite outgrowth, five longest neurites from at least 10 random fields in each well were measured using ImageJ tracing plugin NeuronGrowth (UNAM; *http://www.ifc.unam.mx/ffm/*). The neurite length was defined as the distance between the center of the cell soma and the neurite tip. Incompletely captured neurites missing either the cell body of origin or end point were excluded from analysis. Data obtained from at least three-independent differentiation experiments were used to calculate the average neurite length. Values were expressed as means ± standard error of the mean (S.E.M.).

2.3 *Determination of α-enolase activity*

Determination of α-enolase activity was performed using an ENO1 Human Activity Assay kit (Abcam, Cambridge, U.K.). The preparation of samples and assay procedure was carried out according to the manufacturer's instructions. Briefly, SH-SY5Y cells were washed twice with cold phosphate-buffered saline, harvested by scraping them off the flask and collected by centrifugation (1000 × *g*, 10 min). Cell pellets were lysed in extraction buffer and the protein concentration was estimated by the bicinchoninic acid

(BCA) assay. Samples (0.1 mg/mL) were transferred to a solid assay microplate pre-coated with an alpha-enolase antibody to capture the enzyme. After adding the substrate solution containing 2-phospho-D-glycerate, the absorbance at 340 nm was measured on a 96-well plate reader (Bio-Tek Synergy HT) using a kinetic read mode. The substrate consumption was proportional to NADH depletion, which was reflected by decreased absorbance at 340 nm.

2.4 *Protein extraction for isoelectric focusing*

The cells were harvested by centrifugation (1000 × *g*, 10 min) as described above and stored at −80°C until sample preparation. The cell pellets were resuspended in TE buffer (10 mM TRIS, 1 mM EGTA; pH 7.5) containing protease inhibitors (cOmplete^{TM} protease inhibitor cocktail, Roche) and sonicated 10 times with 5 s burst at 60% amplitude using an ultrasonic converter (Bandelin UW 2070). The lysates were centrifuged at 3000 × *g* for 5 min (4°C). The total protein content in cell lysates was quantified with the BCA assay. Three-independent biological replicates of each condition were used in the experiments. Samples (1 mg of protein) were precipitated with ice-cold acetone and further treated according to the protocol previously described in detail (Ujcikova *et al.* 2016). Finally, the samples were loaded into the reswelling tray.

2.5 *Two-dimensional electrophoresis*

pH 3-11 NL immobilized pH gradient gel strips with 13 cm were rehydrated overnight in the sample-containing rehydration solution in an Immobiline DryStrip reswelling tray (GE Healthcare). Isoelectric focusing was carried out at 14°C using a Multiphor II unit (GE Healthcare) (Manakov *et al.* 2016). The voltage was increased stepwise from 150 (2 h) to 500 V (1 h), then to 3500 V (12 h) and finally to 500 V (3 h). Prior to second-dimensional sodium dodecyl sulfate-polyacrylamide gel electrophoresis (SDS-PAGE), the strips were rinsed with ultrapure water, dried quickly on filter paper and equilibrated in equilibration buffer containing 1% dithiothreitol (DTT). Afterwards, the strips were equilibrated for 10 min in equilibration buffer containing 2.5% iodoacetamide (IAA). Prior to electrophoresis, the strips were overlayed with 0.5% agarose. SDS-PAGE was run in a vertical position at a constant current of 90 mA until the bromophenol blue marker dye reached the end of the gel. The apparatus was cooled to 15°C using the Hoefer SE 600 Unit (GE Healthcare).

2.6 *Staining of 2D gels by colloidal Coomassie Brilliant Blue (CBB) G-250 and image analysis*

For mass spectrometry (MS) analysis, the fresh 2D gels were immediately fixed by soaking for 1 h in fixing solution (50% methanol and 7% glacial acetic acid) and then incubated in colloidal CBB G-250 staining solution (17% ammonium sulphate, 34% methanol, 3% orthophosphoric acid and 0.1% Coomassie G-250) overnight with gentle agitation according to Fountoulakis *et al.* (Fountoulakis *et al.* 1999). Destaining was performed using ultrapure sterile water. CBB-stained gels were stored in 1% acetic acid at 4°C.

Gels were scanned using an Epson Perfection 4990 photo desktop scanner and quantification of spot densities was performed using PDQuest software (Bio-Rad, version 7.3.1) as described previously (Ujcikova *et al.* 2016). At least three replicates were performed for each sample. Proteins that changed in abundance by at least two-fold (Student's *t*-test, $p<0.05$) were selected for mass spectrometric analysis.

2.7 *Protein identification by matrix-assisted laser desorption/ionization-time-of-flight (MALDI-TOF)/MS-MS*

The preparation of samples and their analyses by MALDI-TOF/MS-MS were performed according to the previously described protocols (Ujcikova *et al.* 2014, 2016). Selected CBB-stained spots were cut out of the gels, chopped into small pieces, placed into microtubes and mixed with buffer A (50 mM ammonium bicarbonate and 50 mM DTT in 50% acetonitrile). After sonication for 5 min, the supernatant was discarded and the gel pieces were mixed with buffer A containing 50 mM IAA and sonicated again. The supernatant was discarded, replaced with buffer A containing 50 mM DTT and the samples were sonicated third time to remove excess of IAA. The supernatant was discarded and the samples were again sonicated for 5 min in ultrapure water. The water was then discarded and samples were sonicated for another 5 min in acetonitrile. After discarding acetonitrile, trypsin (5 ng in 10 μL of 50 mM buffer A) was added to the gel pieces and incubated overnight at 37°C. Afterwards, proteolysis was quenched by addition of trifluoroacetic acid and acetonitrile at a final concentration of 1 and 30%, respectively. After 10 min of sonication, a 0.5 mL aliquot of trypsin digest was transferred onto the MALDI target and allowed to dry. Subsequently, a small drop of alpha-cyano-hydroxycinnamic acid solution (2 mg/mL in 80% acetonitrile) was deposited on the area containing the dried trypsin digest and allowed to dry. MALDI-TOF/MS-MS measurements were performed on a 4800 Plus MALDI-TOF/TOF analyzer (Applied Biosystems/MDS Sciex) equipped with a Nd:YAG laser (355 nm, firing rate 200 Hz).

The data were analyzed using in-house running Mascot server 2.2.07 and matched against the comprehensive Uni_human_reviewed database (20273 sequences; 11324606 residues). Database search criteria are as follows: enzyme = trypsin; taxonomy = Homo sapiens (Human). Cysteine carbamidomethylation, methione oxidation and deamidation (NQ) were set as fixed or variable modifications, respectively. The maximum two-missed cleavages were allowed. Only hits that were scored as significant

(MASCOT score ≥ 56, $p<0.05$) were accepted. Protein scores were derived from ion scores as a non-probabilistic basis for ranking protein hits.

2.8 *Gel electrophoresis and western blot analysis*

The relative levels of selected proteins were determined by western blotting. Cells were harvested by centrifugation (1000 × *g*, 10 min). The cell pellet was resuspended in Tris-[hydroxylmethyl]-methyl-2-aminoethane sulfonic acid buffer (20 mM Tris, 3 mM $MgCl_2$, 1 mM ethylenediaminetetraacetic acid, 250 mM sucrose; pH 7.4) in the presence of protease inhibitors (cOmplete™ protease inhibitor cocktail, Roche) and homogenized with a syringe and needle (20 strokes). Cell homogenates were then sonicated three times with 5 s burst at 60% amplitude using an ultrasonic converter (Bandelin UW 2070). Samples were solubilized in Laemmli buffer and loaded (10 μg per line) on 10% polyacrylamide gels for sodium dodecyl sulfate polyacrylamide gel electrophoresis. After electrophoresis, the resolved proteins were electrotransferred onto a nitrocellulose membrane. After blocking in non-fat milk (5%) in Tris-buffered saline with Tween 20 (TBS-T) buffer (10 mM Tris, 150 mM NaCl, 1% (v/v) Tween 20; pH 8.0) for 1 h, membranes were incubated with primary antibodies on an orbital shaker (overnight at 4°C). After three brief wash cycles in TBS-T, the secondary horseradish peroxidase-labeled antibody was applied for 1 h. After another three brief washes (10 min each) in TBS-T, the blots were visualized by enhanced chemiluminescence according to the manufacturer's instructions (Pierce Biotechnology). The immunoblots were scanned and quantitatively analyzed by using ImageQuant™ TL software (Amersham Biosciences). Glyceraldehyde-3-phosphate dehydrogenase (GAPDH) was used as a loading control for protein normalization.

3. Results

3.1 *RA promotes neuronal differentiation of SH-SY5Y cells*

Differentiation of SH-SY5Y cells into a neuronal phenotype was induced by RA following the previously described protocol (Ammer and Schulz 1994). Phase-contrast microscopy was used to inspect the SH-SY5Y cell morphology in order to validate the differentiation procedure. UC SH-SY5Y cells typically tended to grow in clusters and were characterized by non-polarized cell bodies with few truncated processes. Prolonged exposure of SH-SY5Y cells to RA led to neuronal differentiation and most of the cells adopted a typical neuronal morphology. Upon RA treatment, the cells became elongated and displayed a reduction of the cell body and extension of neurites. To monitor the extent of neuronal differentiation, the neurite outgrowth was traced and measured using ImageJ software with NeuronGrowth plugin. The length of neurites increased due to the RA treatment more than two-fold (figure 1A and B).

Changes in the expression of specific markers of UC neuroblastoma cells and neuron-like cells during the differentiation process were monitored by western blotting. However, there was a significant increase in the content of the neuronal marker MAP2, NSE and SNP, as well as in the dopaminergic neuron-specific marker tyrosine hydroxylase (TH) in differentiated cells, the expression level of neural progenitor cell marker nestin was diminished in these cells (figure 1C and D). Both UC and RA-DC SH-SY5Y cells were positive for PCNA and GAP43, and only a slight tendency towards decreased or increased expression, respectively, of these proteins was noted in neuronally differentiated cells.

3.2 *Proteome changes associated with differentiation of SH-SY5Y cells*

Our first set of proteomic experiments were designed to assess the changes in the proteome of SH-SY5Y cells exposed to 10 μM RA for 6 days. Representative gel images of proteins from control (untreated) and RA-treated cells resolved by two-dimensional gel electrophoresis are shown in figure 2. Differential proteomic analysis revealed the quantitative changes in optical density of 17 spots between samples from control and RA-treated cells. To identify the differentially expressed proteins, relevant protein spots were excised from the gels and subjected to MS analysis. This analysis led to the identification of 15 proteins. Two proteins were each detected in two spots (alpha-enolase and t-complex protein 1 subunit gamma (TCP1)). Neuronal differentiation was accompanied by a 3.3-fold up-regulation of one protein (complement component 1 Q subcomponent-binding protein, mitochondrial; C1qbp). Fourteen other proteins were concomitantly down-regulated 2- to 3.7-fold (actin, cytoplasmic 1; alpha-enolase; chromobox protein homolog 1 (CBX1); 14-3-3 protein zeta/delta; nucleophosmin; heterogeneous nuclear ribonucleoproteins (hnRNPs) C1/C2; nucleoside diphosphate kinase A; 60S acidic ribosomal protein P0; TCP1; stress-induced-phosphoprotein 1; hnRNP L; phosphoglycerate mutase 1 (PGM1); poly(rC)-binding protein 1; peroxiredoxin-1), compared to undifferentiated cells (table 1). Differentially expressed proteins were involved to cell signaling, metabolism, apoptosis, antioxidant mechanisms, RNA processing, protein folding and cytoskeleton regulation. Most of these proteins were prevalently localized in the cytosol or the nucleus (table 2, supplementary figure 1). A complete listing of all peptides is provided in supplementary table 1.

3.3 *Effect of rhein on protein expression in SH-SY5Y cells*

In the next set of experiments, we explored the effect of 24 h treatment with 10 μM rhein on protein expression in both UC and RA-DC SH-SY5Y cells. Representative

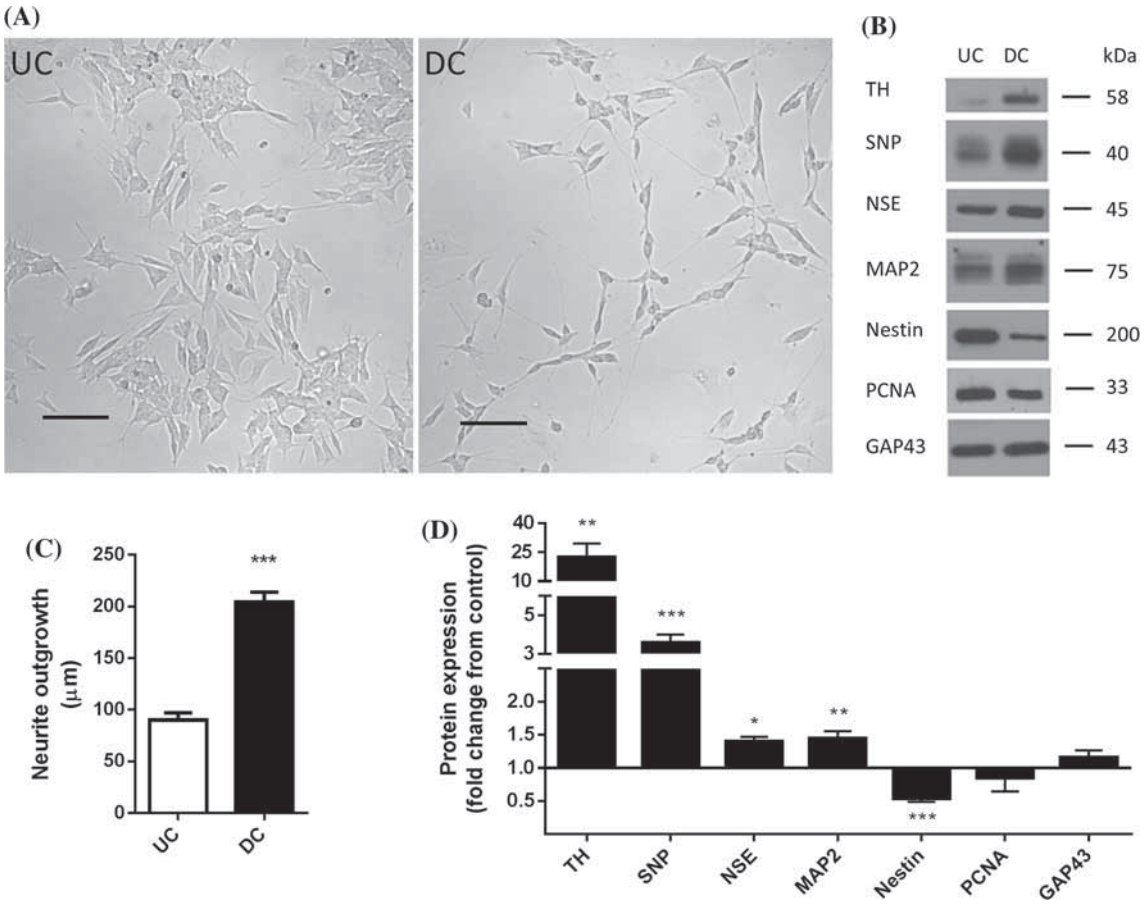

Figure 1. Effects of long-term RA treatment on the cellular morphology and expression of neuronal differentiation markers in SH-SY5Y cells. (**A**) Phase contrast microscopy (magnification 200×) of UC and DC SH-SY5Y cells after 6 days of incubation with 10 μM RA. Scale bars, 100 μm. (**B**) Neurite outgrowth initiated by RA was quantified using ImageJ software with NeuronGrowth plugin. (**C**) Representative western blots showing expression of TH, SNP, nestin, MAP2, NSE, GAP43 and PCNA in UC and DC SH-SY5Y cells. (**D**) The bands were quantified by densitometry and the bar graph shows the fold changes of protein levels after neuronal differentiation. The values were normalized with respect to GAPDH expression. Error bars represent S.E.M. (n = 5) from three-independent experiments. Student's t-test (unpaired) was used to assess statistical significance (*p<0.05, **p<0.01, ***p<0.001).

two-dimensional gel maps of SH-SY5Y cell proteome before and after treatment with rhein are shown in figure 3. Differential proteomic analysis revealed 8 spots with altered density in samples from undifferentiated cells (figure 3A) and 12 spots with altered density in samples from DC SH-SY5Y cells (figure 3B) treated with rhein. The differentially expressed proteins were identified by MS. In this way, 15 proteins were identified and all of them were down-regulated at least 2-fold by treatment with rhein (tables 3 and 4). These proteins are involved in cellular metabolism, cytoskeleton organization, transcriptional and translational regulation and antioxidant defense (supplementary figure 2). Subcellular localization and biological functions of these proteins are described in detail in tables 5 and 6. The comparative proteomic analysis indicated that rhein affected the expression of different proteins in UC and DC SH-SY5Y cells. The only overlapping changes concerned the cytoskeletal proteins actin and beta tubulin. A complete listing of all peptides is provided in supplementary tables 2 and 3.

3.4 *Validation of differential protein expression*

To corroborate the results obtained from 2-DE and MS analysis, the relative abundance of selected proteins linked either to cytoskeleton (α-tubulin), metabolism (α-enolase, GRP 75) or antioxidant mechanisms (peroxiredoxin III (PRX III) and peroxiredoxin VI (PRX VI)) was assessed by western blotting (figure 4). The results of these experiments indicated that RA-induced differentiation of SH-SY5Y cells and/or treatment of these cells with rhein was associated with identical trends (down-regulation) in the expression of these proteins. The content of α-enolase was lower by about 40% in differentiated than in UC SH-SY5Y cells. Rhein markedly (by about 70%) reduced the expression of α-tubulin in both UC and DC SH-SY5Y cells. The levels of GRP 75, PRX III and PRX VI dropped by about 15–45% in RA-DC cells due to treatment with rhein. These findings are similar to those obtained by the preceding quantitative proteomic analysis.

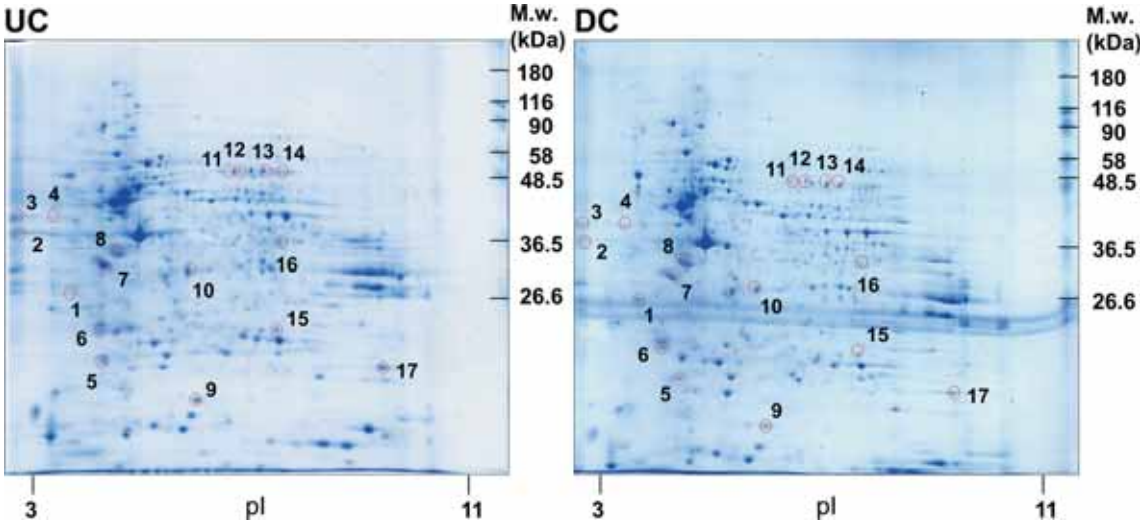

Figure 2. Representative CBB-stained 2-DE gel images of protein expression in UC and DC SH-SY5Y cells. Cells were incubated with 10 μM RA for 6 days in order to induce neuronal differentiation. Samples of cell lysates were resolved by 2-DE and stained with CBB. Red circles indicate spots that underwent statistically significant changes in protein abundance following prolonged treatment with RA. These spots were excised from the gels for MS analysis.

Table 1. List of differentially expressed proteins in neuronally differentiated *vs* undifferentiated SH-SY5Y cells identified by MALDI-TOF MS/MS analysis of CBB-stained gel spots *

Spot	Accession number	Protein name	Mascot score	Matched peptides	SC[a] [%]	MW[b] (kDa)	pI[c]	Change (fold)	p value
1	C1QBP_HUMAN	Complement component 1 Q subcomponent-binding protein, mitochondrial	219	11	31	31.7	4.74	↑ 3.3	0.0028
2	ACTB_HUMAN	Actin, cytoplasmic 1	186	15	26	42.1	5.29	↓ 2.9	0.0024
3	ENOA_HUMAN	Alpha-enolase	78	7	8	47.5	7.01	↓ 2.1	0.0272
4	ENOA_HUMAN	Alpha-enolase	88	6	6	47.5	7.01	↓ 3.7	0.0008
5	CBX1_HUMAN	Chromobox protein homolog 1	75	17	64	21.5	4.85	↓ 3.2	0.0243
6	1433Z_HUMAN	14-3-3 protein zeta/delta	152	14	21	27.9	4.73	↓ 2.1	0.0013
7	NPM_HUMAN	Nucleophosmin	164	15	29	32.7	4.64	↓ 2.0	0.0297
8	HNRPC_HUMAN	Heterogeneous nuclear ribonucleoproteins C1/C2	204	19	35	33.7	4.95	↓ 3.2	0.0205
9	NDKA_HUMAN	Nucleoside diphosphate kinase A	281	16	44	17.3	5.83	↓ 2.3	0.0009
10	RLA0_HUMAN	60S acidic ribosomal protein P0	267	14	26	34.4	5.71	↓ 2.3	0.0342
11	TCPG_HUMAN	T-complex protein 1 subunit gamma	174	6	6	61.1	6.10	↓ 2.3	0.0303
12	TCPG_HUMAN	T-complex protein 1 subunit gamma	200	8	8	61.1	6.10	↓ 2.3	0.0276
13	STIP1_HUMAN	Stress-induced-phosphoprotein 1	295	21	17	63.2	6.40	↓ 2.2	0.0015
14	HNRPL_HUMAN	Heterogeneous nuclear ribonucleoprotein L	251	19	15	64.7	8.46	↓ 3.0	0.0407
15	PGAM1_HUMAN	Phosphoglycerate mutase 1	274	14	36	28.9	6.67	↓ 2.6	0.0073
16	PCBP1_HUMAN	Poly(rC)-binding protein 1	236	15	28	38.0	6.66	↓ 2.3	0.0021
17	PRDX1_HUMAN	Peroxiredoxin-1	619	24	59	22.3	8.27	↓ 2.1	0.0020

[a] sequence coverage, [b] theoretical molecular weight, [c] theoretical isoelectric point

* Please refer to supplementary table 1 for a complete list of peptides.

3.5 *Rhein treatment interferes with RA-induced differentiation of SH-SY5Y cells*

To investigate the impact of rhein on SH-SY5Y cell differentiation, the cells were incubated in the presence of 10 μM rhein for 24 h before addition of RA. After 6 days of co-incubation with rhein and RA, there was no observable cell clustering. The cells thus represented an appearance partially similar to that seen during RA-induced differentiation, yet there was a less pronounced cell stretching and reduced neurite outgrowth. The medium neurite length was rather increased but it was less than that observed in the absence of rhein in RA-treated cells (supplementary figure 3). Analysis of neuronal markers revealed specific changes in their

Table 2. Subcellular localization and biological functions of altered proteins in neuronally differentiated *vs* undifferentiated SH-SY5Y cells identified by MALDI-TOF MS/MS analysis of CBB-stained gel spots

Spot	Accession number	Protein name	Change (fold)	Subcellular localization	Molecular functions and cellular processes
1	C1QBP_HUMAN	Complement component 1 Q subcomponent-binding protein, mitochondrial	↑ 3.3	mitochondrion matrix, nucleus, cell membrane	adaptive immunity, apoptosis, transcription
2	ACTB_HUMAN	Actin, cytoplasmic 1	↓ 2.9	cytoplasm, cytoskeleton	ATP binding, membrane organization
3,4	ENOA_HUMAN	Alpha-enolase	↓ 2.1, ↓ 3.7	cytoplasm, cell membrane	glycolysis, gluconeogenesis
5	CBX1_HUMAN	Chromobox protein homolog 1	↓ 3.2	nucleus	chromatin binding, enzyme binding
6	1433Z_HUMAN	14-3-3 protein zeta/delta	↓ 2.1	cytoplasm	adapter protein, signal transduction
7	NPM_HUMAN	Nucleophosmin	↓ 2.0	nucleus, cytoplasm	chaperone, cell aging, signal transduction
8	HNRPC_HUMAN	Heterogeneous nuclear ribonucleoproteins C1/C2	↓ 3.2	nucleus	ribonucleoprotein, mRNA processing
9	NDKA_HUMAN	Nucleoside diphosphate kinase A	↓ 2.3	cytoplasm, nucleus	cell proliferation, signal transduction, nucleotide metabolism
10	RLA0_HUMAN	60S acidic ribosomal protein P0	↓ 2.3	nucleus, cytoplasm	ribonucleoprotein, translation
11,12	TCPG_HUMAN	T-complex protein 1 subunit gamma	↓ 2.3, ↓ 2.3	cytoplasm	chaperone, ATP binding
13	STIP1_HUMAN	Stress-induced-phosphoprotein 1	↓ 2.2	cytoplasm, nucleus	co-chaperone, response to stress, RNA binding
14	HNRPL_HUMAN	Heterogeneous nuclear ribonucleoprotein L	↓ 3.0	nucleus, cytoplasm	ribonucleoprotein, RNA processing
15	PGAM1_HUMAN	Phosphoglycerate mutase 1	↓ 2.6	cytoplasm	glycolysis
16	PCBP1_HUMAN	Poly(rC)-binding protein 1	↓ 2.3	nucleus, cytoplasm	ribonucleoprotein, mRNA splicing
17	PRDX1_HUMAN	Peroxiredoxin-1	↓ 2.1	cytoplasm	antioxidant, cell proliferation

expression during the differentiation process. TH, SNP, NSE and PCNA exhibited similar trends in expression to those observed in RA-DC cells. Interestingly, the cytoskeletal proteins MAP2 and GAP43 displayed an opposite expression tendency and were down-regulated, in contrast to both UC and RA-DC cells (supplementary figure 3). Nestin expression levels remained basically unchanged.

In another set of experiments, we focused on α-enolase, a key glycolytic enzyme that may play an important role in the process of cell differentiation. The expression of α-enolase was markedly lower in RA-DC than in UC SH-SY5Y cells and treatment with rhein strongly prevented the enzyme down-regulation (figure 5A). Similar data were obtained by monitoring α-enolase activity, i.e., the drop in enzyme activity observed in the course of RA-induced cell differentiation was abolished in the presence of rhein (figure 5B).

4. Discussion

The SH-SY5Y neuroblastoma cell line represents one of the most widely used models to study *in vitro* neuronal functions and cellular behavior. These cells may exist in both the undifferentiated and differentiated states. In the present study we employed 2-DE/MS comparative proteomic approach to examine the impact of a natural anticancer agent rhein on the proteome of both UC and RA-DC SH-SY5Y cells. A great deal of attention was also devoted to delineating the presumed effect of rhein on the process of cellular differentiation and to changes in protein expression during the RA-induced differentiation.

4.1 *The proteome of SH-SY5Y cells is affected by RA-induced differentiation*

In spite of numerous studies conducted with SH-SY5Y cells, there is still a controversy about the phenotype of neuronally DC SH-SY5Y cells (Hashemi *et al.* 2003; Korecka *et al.* 2013). Therefore, we first aimed to describe major proteomic changes in these cells under our experimental conditions and compare the obtained results with previously published proteomic data regarding RA-DC SH-SY5Y cells. Besides detecting expression alterations in several proteins previously described in the literature we identified some differentially regulated proteins that have not yet been reported. The proteins whose levels changed upon RA treatment participate in distinct aspects of neuronal differentiation,

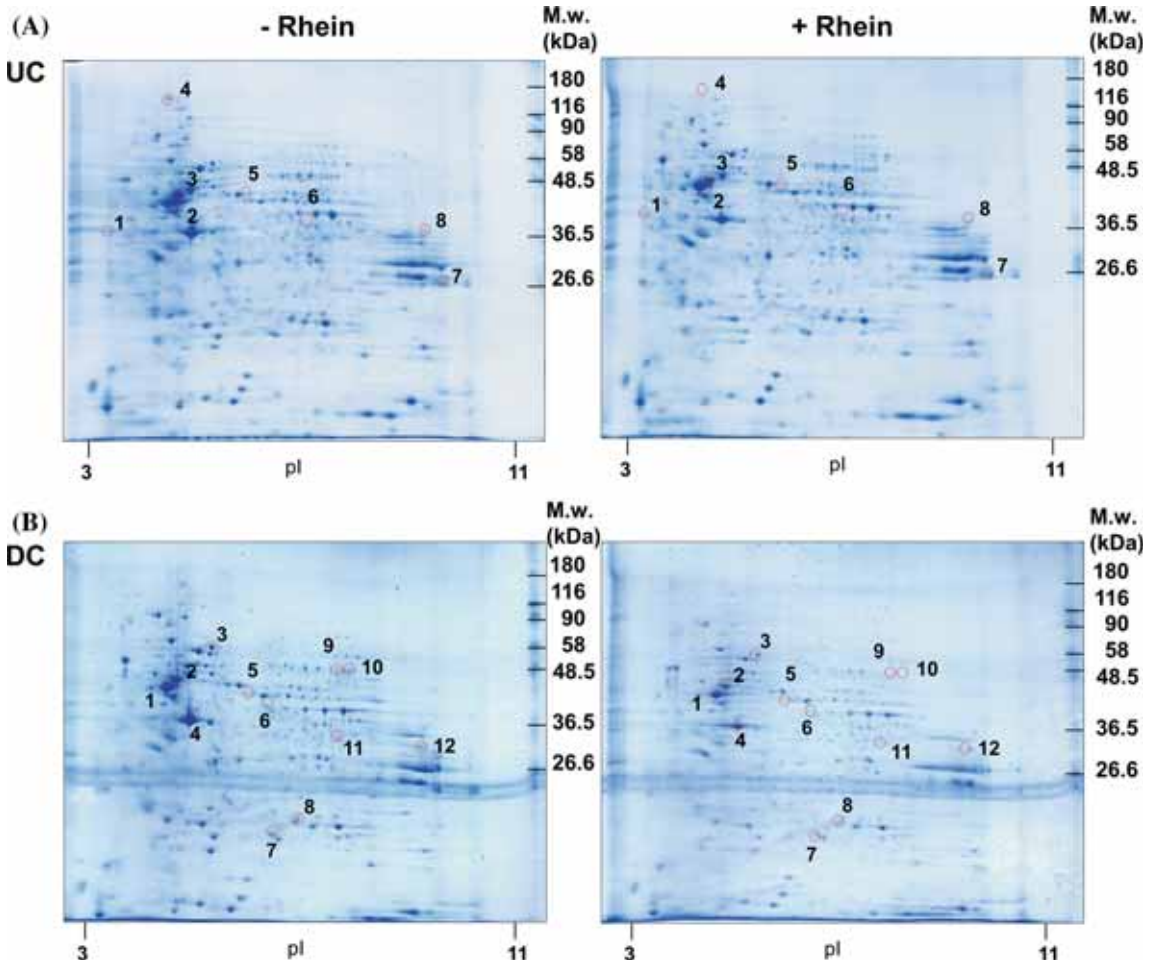

Figure 3. Effect of rhein on protein expression in SH-SY5Y cells. Representative CBB-stained 2-DE gel images of proteins expressed in undifferentiated and differentiated SH-SY5Y cells either untreated or treated with rhein. (**A**) Undifferentiated cells, (**B**) differentiated cells, left panel: untreated cells, right panel: rhein treated cells. Undifferentiated and differentiated cells were incubated with 10 μM rhein for 24 h. Samples of cell lysates were resolved by 2-DE and stained with CBB. Red circles indicate spots that underwent statistically significant changes in protein abundance after 24 h treatment with rhein. These spots were excised from gels for MS analysis.

Table 3. List of differentially expressed proteins by rhein in undifferentiated SH-SY5Y cells identified by MALDI-TOF MS/MS analysis of CBB-stained gel spots *

Spot	Accession number	Protein name	Mascot score	Matched peptides	SC[a] [%]	MW[b] (kDa)	pI[c]	Change (fold)	p value
1	ACTB_HUMAN	Actin, cytoplasmic 1	264	16	22	42.1	5.29	↓ 2.5	0.0404
2	TBB5_HUMAN	Tubulin beta chain	532	39	50	50.1	4.78	↓ 6.2	0.0392
3	TBA1A_HUMAN	Tubulin alpha-1A chain	306	27	45	50.8	4.94	↓ 2.1	0.0054
4	TBB5_HUMAN	Tubulin beta chain	376	24	29	50.1	4.78	↓ 5.2	0.0477
5	PDIA3_HUMAN	Protein disulfide-isomerase A3	213	21	21	57.1	5.98	↓ 2.7	0.0429
6	ACTZ_HUMAN	Alpha-centractin	64	6	9	42.7	6.19	↓ 2.8	0.0246
7	ROA1_HUMAN	Heterogeneous nuclear ribonucleoprotein A1	404	31	44	38.8	9.17	↓ 3.9	0.0348
8	THIM_HUMAN	3-ketoacyl-CoA thiolase, mitochondrial	153	12	13	42.3	8.32	↓ 3.6	0.0375

[a] sequence coverage, [b] theoretical molecular weight, [c] theoretical isoelectric point

* Please refer to supplementary table 2 for a complete list of peptides.

Table 4. Subcellular localization and biological functions of proteins altered by rhein in undifferentiated SH-SY5Y cells

Spot	Accession number	Protein name	Change (fold)	Subcellular localization	Molecular functions and cellular processes
1	ACTB_HUMAN	Actin, cytoplasmic 1	↓ 2.5	cytoplasm, cytoskeleton	ATP binding, membrane organization
2,4	TBB5_HUMAN	Tubulin beta chain	↓ 6.2, ↓ 5.2	cytoplasm, cytoskeleton	GTP binding, microtubule-based process, cell division
3	TBA1A_HUMAN	Tubulin alpha-1A chain	↓ 2.1	cytoplasm, cytoskeleton	GTP binding, microtubule-based process, cell division
5	PDIA3_HUMAN	Protein disulfide-isomerase A3	↓ 2.7	endoplasmic reticulum	formation and breakage of disulfide bonds, protein folding
6	ACTZ_HUMAN	Alpha-centractin	↓ 2.8	cytoplasm, cytoskeleton, centrosome	ATP-binding, vesicle-mediated transport
7	ROA1_HUMAN	Heterogeneous nuclear ribonucleoprotein A1	↓ 3.9	nucleus, cytoplasm	ribonucleoprotein, mRNA splicing
8	THIM_HUMAN	3-ketoacyl-CoA thiolase, mitochondrial	↓ 3.6	mitochondrion	fatty acid metabolism, transit peptide

Table 5. List of differentially expressed proteins by rhein in neuronally differentiated SH-SY5Y cells identified by MALDI-TOF MS/MS analysis of CBB-stained gel spots *

Spot	Accession number	Protein name	Mascot score	Matched peptides	SC[a] [%]	MW[b] (kDa)	pI[c]	Change (fold)	p value
1	TBB5_HUMAN	Tubulin beta chain	562	40	64	50.1	4.78	↓ 2.5	0.0124
2	TBA1B_HUMAN	Tubulin alpha-1B chain	391	31	57	50.8	4.94	↓ 2.5	0.0282
3	GRP75_HUMAN	Stress-70 protein, mitochondrial	588	30	35	73.9	5.87	↓ 2.3	0.0358
4	ACTB_HUMAN	Actin, cytoplasmic 1	393	26	47	42.1	5.29	↓ 3.3	0.0075
5	HNRH1_HUMAN	Heterogeneous nuclear ribonucleoprotein H	174	16	23	49.5	5.89	↓ 4.4	0.0229
6	HNRH1_HUMAN	Heterogeneous nuclear ribonucleoprotein H	131	10	16	49.5	5.89	↓ 2.7	0.0122
7	PRDX3_HUMAN	Thioredoxin-dependent peroxide reductase, mitochondrial	304	11	19	28.0	7.67	↓ 2.6	0.0126
8	PRDX6_HUMAN	Peroxiredoxin-6	322	14	40	25.1	6.00	↓ 2.7	0.0435
9	HNRPL_HUMAN	Heterogeneous nuclear ribonucleoprotein L	164	20	15	64.7	8.46	↓ 2.5	0.0455
10	HNRPL_HUMAN	Heterogeneous nuclear ribonucleoprotein L	106	14	11	64.7	8.46	↓ 2.8	0.0058
11	PCBP1_HUMAN	Poly(rC)-binding protein 1	139	8	13	38.0	6.66	↓ 4.9	0.0215
12	ALDOA_HUMAN	Fructose-bisphosphate aldolase A	266	18	34	39.9	8.30	↓ 2.4	0.0449

[a] sequence coverage, [b] theoretical molecular weight, [c] theoretical isoelectric point

* Please refer to supplementary table 3 for a complete list of peptides.

including energy production and utilization, cytoskeleton regulation, protein synthesis and folding, cell signaling, proliferation and self-protection.

Nucleophosmin, stress induced phosphoprotein 1 and CBX1 have all been reported to be highly expressed in cancer cells promoting their proliferation ability (Chao *et al.* 2013; Wong *et al.* 2013; Lee *et al.* 2015). In accordance with our current results, the expression levels of these proteins were reduced upon treatment with differentiation-promoting reagents (Baharvand *et al.* 2008; XU *et al.* 2014; Mattout *et al.* 2015). We also detected down-regulation of peroxiredoxin-1 (PRX1) and 14-3-3 protein zeta/delta, multifunctional proteins involved in mitochondrial integrity, apoptosis, cell growth, metabolism and survival functions (Kleppe *et al.* 2011). Changes in PRX1 levels were repeatedly observed during tumor cell or neuron differentiation (Kim *et al.* 2008; Yan *et al.* 2009; Sun *et al.* 2015). Interestingly, expression of peroxiredoxins is very low in the dopaminergic neurons in several brain regions (Goemaere and Knoops 2012).

Some of the proteins differentially regulated in the course of neuronal differentiation belong to a family of hnRNPs. These proteins are involved in the processing of heterogeneous nuclear RNAs into mature mRNAs, as well as in regulation of gene expression and mRNA metabolism. It has been suggested that hnRNPs plays a role in carcinogenesis. Deficient expression of hnRNPs was found to be associated with telomere shortening and oncogenic transformation. hnRNP E1 (poly(rC)-binding protein 1) in particular may contribute to cell proliferation and differentiation

Table 6. Subcellular localization and biological functions of proteins altered by rhein in neuronally differentiated SH-SY5Y cells

Spot	Accession number	Protein name	Change (fold)	Subcellular localization	Molecular functions and cellular processes
1	TBB5_HUMAN	Tubulin beta chain	↓ 2.5	cytoplasm, cytoskeleton	GTP binding, microtubule-based process, cell division
2	TBA1B_HUMAN	Tubulin alpha-1B chain	↓ 2.5	cytoplasm, cytoskeleton	GTP binding, microtubule-based process, cell division
3	GRP75_HUMAN	Stress-70 protein, mitochondrial	↓ 2.3	mitochondrion, nucleus	chaperone, erythropoiesis process
4	ACTB_HUMAN	Actin, cytoplasmic 1	↓ 3.3	cytoplasm, cytoskeleton	ATP binding, membrane organization
5,6	HNRH1_HUMAN	Heterogeneous nuclear ribonucleoprotein H	↓ 4.4, ↓ 2.7	nucleus	ribonucleoprotein, mRNA splicing
7	PRDX3_HUMAN	Thioredoxin-dependent peroxide reductase, mitochondrial	↓ 2.6	mitochondrion	antioxidant, detoxification of reactive oxygen species
8	PRDX6_HUMAN	Peroxiredoxin-6	↓ 2.7	cytoplasm, lysosome	antioxidant, detoxification of reactive oxygen species
9,10	HNRPL_HUMAN	Heterogeneous nuclear ribonucleoprotein L	↓ 2.5, ↓ 2.8	nucleus, cytoplasm	ribonucleoprotein, mRNA splicing
11	PCBP1_HUMAN	Poly(rC)-binding protein 1	↓ 4.9	nucleus, cytoplasm	ribonucleoprotein, mRNA splicing
12	ALDOA_HUMAN	Fructose-bisphosphate aldolase A	↓ 2.4	cytoplasm	glycolysis, scaffolding protein

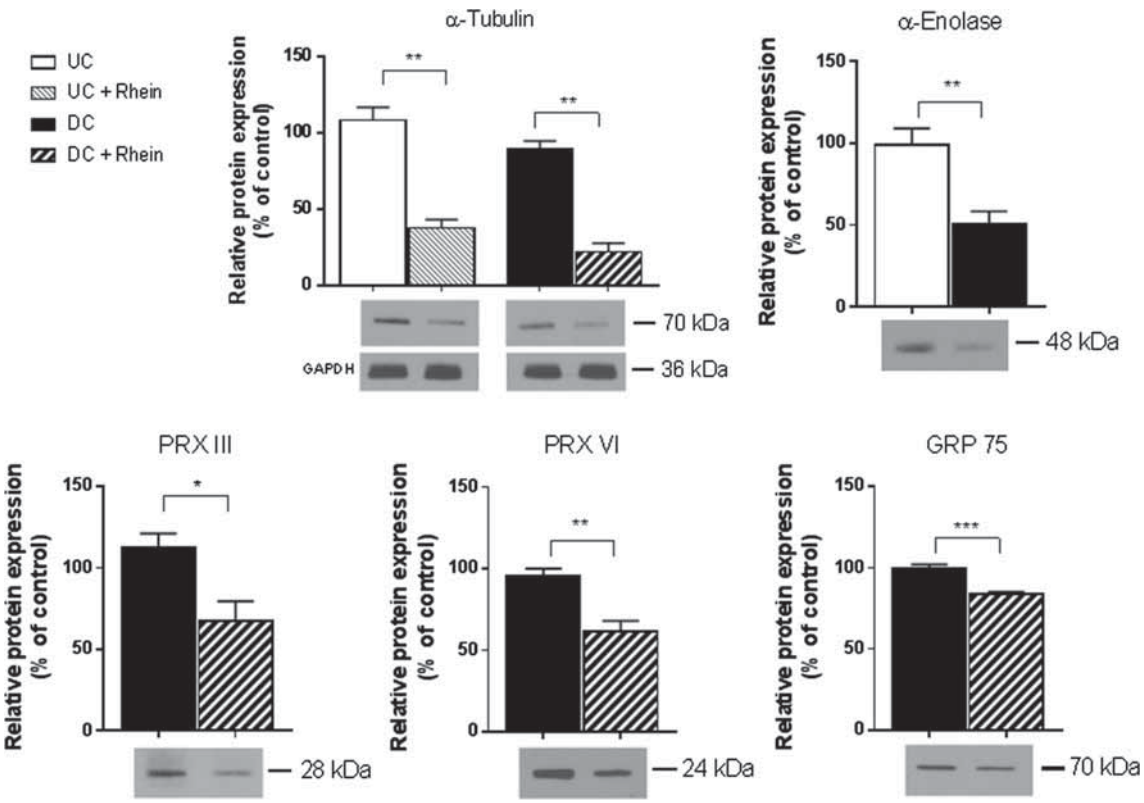

Figure 4. Validation of proteomic data by western blot analysis. The relative expression levels of selected proteins were determined in samples from both UC and DC SH-SY5Y cells either not affected by rhein. GAPDH was used as a loading control. The bands were quantified by densitometry. The bar graphs show the fold changes of the normalized values for each protein. Data are presented as mean ± S.E.M. of three-independent experiments. Student's *t*-test (unpaired) was used to assess the statistical significance (*$p<0.05$, **$p<0.01$, ***$p<0.001$).

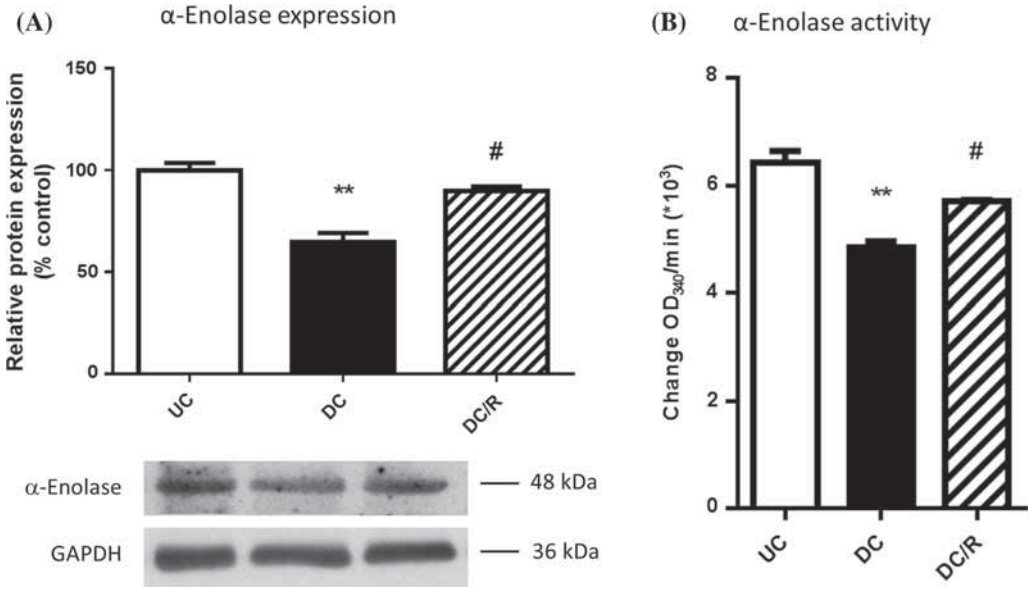

Figure 5. Effect of long-term rhein treatment on α-enolase expression and activity in SH-SY5Y cells. Untreated (UC and RA-DC SH-SY5Y cells were prepared as described in Materials and Methods. SH-SY5Y cells were pretreated with 10 μM rhein for 24 h prior to the addition of 10 μM RA and then cultivated in the presence of both these substances for next 6 days (DC/R). (**A**) Changes in the expression level of α-enolase were assessed by western blotting. The values were normalized to GAPDH and expressed as percent of control (untreated cells, UC). (**B**) Enzyme activity of α-enolase was determined using the ENO1 Human Activity Assay kit and the data are expressed as the change in OD per minute. The error bars represent S.E.M. of three-independent experiments. Student's *t*-test (unpaired) was used to assess statistical significance (**$p<0.01$ *vs* UC, #$p<0.05$ *vs* DC).

(Chaudhury *et al.* 2010). Individual hnRNPs might have potential roles in neural cell differentiation and function (Licatalosi *et al.* 2012; Sinnamon *et al.* 2012; Folci *et al.* 2014). Interestingly, vimentin (Vm) is a common partner for hnRNP C1/C2 (Kanlaya *et al.* 2010). Vm is initially expressed by early neuronal precursors and it is essential for neuritogenesis at least in culture. Vm is gradually replaced with neurofilaments during cell differentiation because of the down-regulation of its expression (Yabe *et al.* 2003). We also noticed a drop in the content of 60S acidic ribosomal protein P0 and TCP1, which mirrors lower protein synthesis and folding. Birkeland *et al.* used selective cAMP analogs to induce SH-SY5Y neuroblastoma differentiation and they detected changes (mostly down-regulation) in hnRNPs, including hnRNP L, and in ribosomal proteins (Birkeland *et al.* 2009). On the other hand, PGM1 and PRX1 were up-regulated under these conditions. Cimmino *et al.* identified some differentially regulated hnRNPs upon RA-induced differentiation of LAN-5 neuroblastoma cells (Cimmino *et al.* 2007). Similarly to us, they observed down-regulation of α-enolase. α-Enolase has been reported to be up-regulated in several cancer cell lines where it supports anaerobic proliferation. Furthermore, expression of this enzyme may change depending on metabolic, developmental or pathophysiological conditions of cells. The expression level of α-enolase might also vary at different stages of cell differentiation. It is up-regulated during cell growth and its levels drop during quiescent phases. α-Enolase binds to other glycolytic enzymes and has affinity towards cytoskeletal proteins, including fragments of F-actin and tubulin. It has been shown to associate with centrosomes in HeLa cells (Díaz-Ramos *et al.* 2012).

The only up-regulated protein we found, complement component 1 Q subcomponent-binding protein (C1qbp), is believed to be a multifunctional and multicompartmental protein with function in various processes, including proliferation, apoptosis (McGee *et al.* 2011), ribosome biogenesis (Yoshikawa *et al.* 2011) and pre-mRNA splicing regulation (Petersen-Mahrt *et al.* 1999). Interestingly, C1qbp has been implicated in tumor cell metabolism and survival and it has been shown to be important for the proper function of the mitochondrial oxidative phosphorylation (OXPHOS) system (Li *et al.* 2011). This is consistent with a recent report of Hu *et al.* who demonstrated that knockdown of C1qbp causes mitochondria fragmentation (Hu *et al.* 2013). Knocking down C1qbp expression in human cancer cells strongly shifted their metabolism from OXPHOS to glycolysis. The C1qbp knockdown cells also exhibited reduced synthesis of the mitochondrial DNA-encoded OXPHOS polypeptides (Fogal *et al.* 2010).

It is known that increased rates of glucose uptake and glycolysis are generally found in tumor cells as they depend mostly on glycolytic pathways instead of OXPHOS (Zheng 2012). The observed changes in C1qbp protein and the glycolytic enzymes α-enolase and PGM1 in RA-DC SH-SY5Y cells may represent a shift towards mitochondrial energy production and suppression of the tumorous character of these cells. Actually, neuronally DC SH-SY5Y cells were

reported to have an increased rate of OXPHOS and lower dependence on glycolysis (Xun *et al.* 2012).

4.2 *Rhein alters protein expression in SH-SY5Y cells*

In the next part of the study we investigated the protein expression changes in SH-SY5Y cells exposed to rhein, an antineoplastic drug that has been hypothesized to interfere with tumor cell proliferation by affecting the energy metabolism and mitochondrial function (Legendre *et al.* 2009; Du *et al.* 2013; Mao *et al.* 2017). Our analysis identified a total of 15 down-regulated proteins in samples from SH-SY5Y cells treated with rhein for 24 h. Several cytoskeletal proteins (actin beta, tubulin alpha chain and tubulin beta chain) were similarly regulated in both undifferentiated and RA-differentiated cells. Iosi reported that treatment of A431 cells with rhein resulted in noticeable morphological modifications because the cytoskeletal microfilament system beneath the plasma membrane underwent a rearrangement. These authors pointed out that the cell surface and mitochondria are likely targets in rhein-induced cell damage (Iosi *et al.* 1993).

We also observed that treatment of RA-DC SH-SY5Y with rhein led to the down-regulation of stress-70 protein (GRP75; mortalin). Mortalin is a chaperone protein located in mitochondria where it regulates the import of nuclear-encoded proteins and therefore plays a central role in mitochondrial biogenesis. This protein has been implicated in the control of cell proliferation and cellular aging and it has also an important antiapoptotic function (Dores-Silva *et al.* 2015). Mortalin plays a crucial role in brain which highly utilizes energy and depends heavily on mitochondrial functions (Takano *et al.* 1997). These studies have demonstrated that mortalin-mediated mitochondrial functions are not only the key factors in maintaining the continued proliferation of cancer cells but also in the normal physiology of nerve cells. The lack of functional mortalin could contribute to the development of neurodegenerative diseases.

Another chaperone protein, protein disulfide isomerase A3 (PDI), was found also to be down-regulated following rhein exposure. PDI catalyzes the *in vitro* isomerization of intramolecular disulfide bridges in the endoplasmic reticulum. This chaperon exhibits broad specificity and can catalyze the *in vitro* folding of a variety of proteins (Wang 1998). Protein misfolding is a contributing mechanism to cellular toxicity. In many neurodegenerative diseases there is a link between the accumulation of misfolded proteins inside the neurons to cellular dysfunction and cell death. PDI is up-regulated in animal models and brains of patients with neurological-protein folding diseases. Interestingly, inhibition of PDI in rat brain cells suppressed the toxicity of mutant huntingtin exon 1 and Aβ peptides processed from the amyloid precursor protein. Irreversible inhibition of PDI activity resulted in enhanced protection in cell and organotypic brain slice culture models of Huntington disease (Hoffstrom *et al.* 2010; Kaplan *et al.* 2015).

Other metabolically relevant proteins differentially regulated by rhein were fructose-bisphosphate aldolase A in RA-DC cells and 3-ketoacyl-CoA thiolase in UC SH-SY5Y cells. Fructose-bisphosphate aldolase A plays a key role in glycolysis and gluconeogenesis and contributes to the regulation of cell shape and mobility (Walsh *et al.* 1989; Kusakabe *et al.* 1997). The importance of 3-ketoacyl-CoA thiolase in neuronal energy metabolism is rather speculative because the enzymatic capacity of the β-oxidation in brain mitochondria is markedly lower than in mitochondria from the other high-energy turnover tissues (Yang *et al.* 1987).

Levels of two peroxiredoxins, PRX VI and thioredoxin-dependent peroxide reductase (PRX III) were dramatically decreased after rhein treatment of RA-DC cells. Human peroxiredoxins play important roles in eliminating the accumulated hydrogen peroxide (Netto and Antunes 2016). Oxidative stress induced by reactive oxygen species (ROS) has been implicated in the pathogenesis of several neurodegenerative diseases. Under such detrimental conditions, cytoplasmic peroxiredoxins are usually up-regulated to combat elevated ROS levels (Kim *et al.* 2001). However, decreased protein levels of PRX III, which is exclusively located in mitochondria, could be caused by mitochondrial damage (Chang *et al.* 2004).

hnRNP proteins are multifunctional proteins that can participate in pre-mRNA processing such as splicing and are important determinants of mRNA export, localization, translation and stability (Dreyfuss *et al.* 2002). The expression changes observed in hnRNP H and A1 proteins are particularly interesting because these proteins may regulate alternative splicing of insulin receptor pre-mRNA (Paul *et al.* 2006; Talukdar *et al.* 2011). Insulin signaling in the central nervous system has recently emerged as a novel important field of research because the decreased brain insulin levels and altered signaling were found to be associated with impaired cognitive processes and age-related neurodegenerative diseases (Neth and Craft 2017). Rhein is known for its ability to inhibit RNA m6A demethylase FTO and m6A has recently been identified as a key molecule whose modification by FTO raises the possibility of regulating gene expression and consequently protein translation (Batista 2017). hnRNPs that function as readers on modified RNA may be involved in this translational regulation. Posttranslational modification of mRNA by m6A was shown to alter the mRNA stem-loop structure, and this structural change in turn regulates the interaction between the mRNA molecule and hnRNP C (Liu *et al.* 2015).

4.3 *RA-induced differentiation of SH-SY5Y is hindered by rhein*

SH-SY5Y cells can be differentiated into a neuronal phenotype by long-term exposure to RA. Here, we demonstrated that a 6 day treatment with RA led to SH-SY5Y neuroblastoma differentiation characterized by typical neuron-like

morphological changes, as well as by the protein expression profile of mature neurons. Our next experiments indicated that rhein was able to strongly impede RA-induced differentiation of SH-SY5Y cells. The interfering effect of rhein was manifested by reduced neurite outgrowth and shifted expression of neural markers. Importantly, deregulated differentiation can result in cells with severe functional deficits.

Nestin, an intermediate filament, is expressed in a cell cycle-dependent manner (Sunabori *et al.* 2008). Nestin was found to be down-regulated in neuroepithelial stem cells that ceased dividing and started differentiation (Frederiksen and McKay 1988). In the present study we observed that nestin expression was reduced in RA-DC SH-SY5Y cells and that the presence of rhein prevented this change.

The membrane-associated protein GAP43 is expressed during axonal outgrowth and regeneration. Shea *et al.* showed that GAP43, which is constitutively expressed by neuroblastoma cells, is intensely up-regulated during the initial outgrowth period of neuritogenesis and drops nearly to background levels within hours during continued neurite outgrowth (Shea *et al.* 1991). The MAP2 is a ubiquitous neuronal cytoskeletal protein that binds to tubulin and stabilizes microtubules. MAP2 has also been suggested to promote neuritogenesis because impairment of its microtubules binding ability was shown to reduce neurite numbers in hippocampal neurons (Dehmelt *et al.* 2003) and block neurite initiation in cerebellar macroneurons (Caceres *et al.* 1992). The lower levels of GAP43 and MAP2 detected in cells co-treated with rhein probably contribute to the observed morphological changes.

PCNA was slightly down-regulated in response to RA and the decrement of this protein became even more pronounced in SH-SY5Y cells co-treated with rhein. PCNA levels in tissues have been found to correlate with proliferative activity (Kurki *et al.* 1988). These results suggest that the proliferative ability is decreased in differentiated cells and that rhein might suppress cell proliferation. Similar effects of rhein were also observed in other cell types (Hsia *et al.* 2009; Legendre *et al.* 2009; Aviello *et al.* 2010; Fernand *et al.* 2011). Although rhein was repeatedly reported as an anticancer compound with inhibitory effects on glycolysis, our experiments on SH-SY5Y cells demonstrated that rhein interfered with the diminution of expression and activity of α-enolase. Therefore, it can be suggested that the important metabolic shift towards OXPHOS in differentiating neuroblastoma cells is suppressed under these conditions. Interestingly, Zhang *et al.* reported that rhein is capable of competitive binding to the retinoid X receptor α as a selective antagonist (Zhang *et al.* 2011). However, rhein (Liu *et al.* 2011) and lack of FTO demethylase activity (Zhao *et al.* 2014) were shown to similarly impair adipocyte differentiation, suggesting that rhein's inhibitory action on FTO is responsible for altered-cell differentiation.

5. Conclusions

The present study aimed at comparing proteomic profiles of SH-SY5Y cells affected by rhein. It seems that the cellular differentiation state is of great importance for actual mechanisms triggered by rhein because the expression profiles of proteins in UC and RA-DC SH-SY5Y cells treated with rhein were not identical, except for a few cytoskeletal proteins. Another interesting finding from this study is similar regulation of hnRNP L and hnRNP E1 upon treatment of SH-SY5Y cells with RA and co-treatment with rhein. Our finding showing that rhein interferes with RA-induced differentiation of SH-SY5Y cells support the assumption that the differentiation process itself is affected by this drug. These observations imply that rhein may distort the mechanism of RA action, but other possible factors, like rhein's inhibitory activity on FTO, must also be taken into consideration. These issues deserve further investigation.

Acknowledgements

This study was supported by the Czech Science Foundation (16-21228Y), by the Charles University Grant Agency (898616), by the project no. LQ1605 (MEYS CR, NPU II) and institutional project SVV-260434/2018. PT was a recipient of Primus/SCI/33 grant from Charles University. We appreciate the professional assistance of Karel Harant and Pavel Talacko (Proteomics Core Facility of BIOCEV, Faculty of Science, Charles University) with mass spectrometric analysis.

References

Ammer H and Schulz R 1994 Retinoic acid-induced differentiation of human neuroblastoma SH-SY5Y cells is associated with changes in the abundance of G proteins. *J. Neurochem.* **62** 1310–1318

Aviello G, Rowland I, Gill CI, Acquaviva AM, Capasso F, McCann M, Capasso R, Izzo AA and Borrelli F 2010 Anti-proliferative effect of rhein, an anthraquinone isolated from Cassia species, on Caco-2 human adenocarcinoma cells. *J. Cell. Mol. Med.* **14** 2006–2014

Baharvand H, Fathi A, Gourabi H, Mollamohammadi S and Salekdeh GH 2008 Identification of mouse embryonic stem cell-associated proteins. *J. Proteome Res.* **7** 412–423

Batista PJ 2017 The RNA modification N6-methyladenosine and its implications in human disease. *Genomics Proteomics Bioinf.* **15** 154–163

Biedler JL, Helson L and Spengler BA 1973 Morphology and growth, tumorigenicity, and cytogenetics of human neuroblastoma cells in continuous culture. *Cancer Res.* **33** 2643–2652.

Birkeland E, Nygaard G, Oveland E, Mjaavatten O, Ljones M, Doskeland S O, Krakstad C and Selheim F 2009 Epac-induced alterations in the proteome of human SH-SY5Y neuroblastoma cells. *J. Proteomics Bioinform.* **2** 244–254

Bounda G-A, Zhou W, Wang D and Yu F 2015 Rhein elicits *in vitro* cytotoxicity in primary human liver HL-7702 cells by inducing apoptosis through mitochondria-mediated pathway. *Evid. Based Complement. Altern. Med.* **2015** 1–19

Caceres A, Mautino J and Kosik KS 1992 Suppression of MAP2 in cultured cerebellar macroneurons inhibits minor neurite formation. *Neuron* **9** 607–618

Chang T-S, Cho C-S, Park S, Yu S, Kang SW and Rhee SG 2004 Peroxiredoxin III, a mitochondrion-specific peroxidase, regulates apoptotic signaling by mitochondria. *J. Biol. Chem.* **279** 41975–41984

Chang C-Y, Chan H-L, Lin H-Y, Way T-D, Kao M-C, Song M-Z, Lin Y-J and Lin C-W 2012 Rhein induces apoptosis in human breast cancer cells. *Evid. Based Complement. Altern. Med.* **2012** 952504

Chao A, Lai C-H, Tsai C-L, Hsueh S, Hsueh C, Lin C-Y, Chou H-H, Lin Y-J, Chen H-W, Chang T-C and Wang T-H 2013 Tumor stress-induced phosphoprotein1 (STIP1) as a prognostic biomarker in ovarian cancer. *PLoS One* **8** e57084

Chaudhury A, Chander P and Howe PH 2010 Heterogeneous nuclear ribonucleoproteins (hnRNPs) in cellular processes: Focus on hnRNP E1's multifunctional regulatory roles. *RNA* **16** 1449–1462

Chen B, Ye F, Yu L, Jia G, Huang X, Zhang X, Peng S, Chen K, Wang M, Gong S, Zhang R, Yin J, Li H, Yang Y, Liu H, Zhang J, Zhang H, Zhang A, Jiang H, Luo C and Yang CG 2012 Development of cell-active N6-methyladenosine RNA demethylase FTO inhibitor. *J. Am. Chem. Soc.* **134** 17963–17971

Cheung Y-T, Lau W K-W, Yu M-S, Lai C S-W, Yeung S-C, So K-F and Chang R C-C 2009 Effects of all-trans-retinoic acid on human SH-SY5Y neuroblastoma as *in vitro* model in neurotoxicity research. *Neurotoxicology* **30** 127–135

Cimmino F, Spano D, Capasso M, Zambrano N, Russo R, Zollo M and Iolascon A 2007 Comparative proteomic expression profile in all-trans retinoic acid differentiated neuroblastoma cell line. *J. Proteome Res.* **6** 2550–2564

Cuende J, Moreno S, Bolaños JP and Almeida A 2008 Retinoic acid downregulates Rae1 leading to APCCdh1 activation and neuroblastoma SH-SY5Y differentiation. *Oncogene* **27** 3339–3344

Dehmelt L, Smart F M, Ozer RS and Halpain S 2003 The role of microtubule-associated protein 2c in the reorganization of microtubules and lamellipodia during neurite initiation. *J. Neuroscience* **23** 9479–9490

Díaz-Ramos A, Roig-Borrellas A, García-Melero A and López-Alemany R 2012 α-Enolase, a multifunctional protein: Its role on pathophysiological situations. *J. Biomed. Biotechnol.* **2012** 156795

Dores-Silva PR, Barbosa LRS, Ramos CHI and Borges JC 2015 Human mitochondrial Hsp70 (mortalin): Shedding light on ATPase activity, interaction with adenosine nucleotides, solution structure and domain organization. *PLoS One* **10** e0117170

Dreyfuss G, Kim VN and Kataoka N 2002 Messenger-RNA-binding proteins and the messages they carry. *Nat. Rev. Mol. Cell Biol.* **3** 195–205

Du Q, Bian X-L, Xu X-L, Zhu B, Yu B and Zhai Q 2013 Role of mitochondrial permeability transition in human hepatocellular carcinoma Hep-G2 cell death induced by rhein. *Fitoterapia* **91** 68–73

Encinas M, Iglesias M, Liu Y, Wang H, Muhaisen A, Ceña V, Gallego C and Comella JX 2000 Sequential treatment of SH-SY5Y cells with retinoic acid and brain-derived neurotrophic factor gives rise to fully differentiated, neurotrophic factor-dependent, human neuron-like cells. *J. Neurochem.* **75** 991–1003

Fernand VE, Losso JN, Truax RE, Villar EE, Bwambok DK, Fakayode SO, Lowry M and Warner IM 2011 Rhein inhibits angiogenesis and the viability of hormone-dependent and -independent cancer cells under normoxic or hypoxic conditions *in vitro*. *Chem. Biol. Interact.* **192** 220–232

Fogal V, Richardson AD, Karmali PP, Scheffler IE, Smith JW and Ruoslahti E 2010 Mitochondrial p32 protein is a critical regulator of tumor metabolism via maintenance of oxidative phosphorylation. *Mol. Cell. Biol.* **30** 1303–1318.

Folci A, Mapelli L, Sassone J, Prestori F, D'Angelo E, Bassani S and Passafaro M 2014 Loss of hnRNP K impairs synaptic plasticity in hippocampal neurons. *J. Neurosci.* **34** 9088–9095

Fountoulakis M, Takács M-F, Berndt P, Langen H and Takács B 1999 Enrichment of low abundance proteins of Escherichia coli by hydroxyapatite chromatography. *Electrophoresis* **20** 2181–2195

Frederiksen K and McKay RD 1988 Proliferation and differentiation of rat neuroepithelial precursor cells *in vivo*. *J. Neurosci.* **8** 1144–1151.

Goemaere J and Knoops B 2012 Peroxiredoxin distribution in the mouse brain with emphasis on neuronal populations affected in neurodegenerative disorders. *J. Comp. Neurol.* **520** 258–280

Hashemi SH, Li J-Y, Ahlman H and Dahlström A 2003 SSR2(a) receptor expression and adrenergic/cholinergic characteristics in differentiated SH-SY5Y cells. *Neurochem. Res.* **28** 449–460

Hoffstrom BG, Kaplan A, Letso R, Schmid RS, Turmel GJ, Lo DC and Stockwell BR 2010 Inhibitors of protein disulfide isomerase suppress apoptosis induced by misfolded proteins. *Nat. Chem. Biol.* **6** 900–906

Hsia TC, Yang JS, Chen GW, Chiu TH, Lu HF, Yang MD, Yu FS, Liu KC, Lai KC, Lin CC and Chung JG 2009 The roles of endoplasmic reticulum stress and Ca2+ on rhein-induced apoptosis in A-549 human lung cancer cells. *Anticancer Res.* **29** 309–318

Hu M, Crawford SA, Henstridge DC, Ng IHW, Boey EJH, Xu Y, Febbraio MA, Jans DA and Bogoyevitch MA 2013 P32 protein levels are integral to mitochondrial and endoplasmic reticulum morphology, cell metabolism and survival. *Biochem. J.* **453** 381–391

Iosi F, Santini MT and Malorni W 1993 Membrane and cytoskeleton are intracellular targets of rhein in A431 cells. *Anticancer Res.* **13** 545–554

Kanlaya R, Pattanakitsakul S, Sinchaikul S, Chen S-T and Thongboonkerd V 2010 Vimentin interacts with heterogeneous nuclear ribonucleoproteins and dengue nonstructural protein 1 and is important for viral replication and release. *Mol. Biosyst.* **6** 795

Kaplan A, Gaschler MM, Dunn DE, Colligan R, Brown LM, Palmer AG, Lo DC and Stockwell BR 2015 Small molecule-induced oxidation of protein disulfide isomerase is neuroprotective. *Proc. Natl. Acad. Sci.* **112** E2245–E2252

Khwanraj K, Phruksaniyom C, Madlah S and Dharmasaroja P 2015 Differential expression of tyrosine hydroxylase protein and apoptosis-related genes in differentiated and undifferentiated SH-SY5Y neuroblastoma cells treated with MPP+. *Neurol. Res. Int.* **2015** 1–11

Kim SH, Fountoulakis M, Cairns N and Lubec G 2001 Protein levels of human peroxiredoxin subtypes in brains of patients with Alzheimer's disease and down syndrome. *J. Neural Transm. Suppl.* **61** 223–235

Kim SY, Kim T J and Lee K-Y 2008 A novel function of peroxiredoxin 1 (Prx-1) in apoptosis signal-regulating kinase 1 (ASK1)-mediated signaling pathway. *FEBS Lett.* **582** 1913–1918

Kleppe R, Martinez A, Døskeland SO and Haavik J 2011 The 14-3-3 proteins in regulation of cellular metabolism. *Semin. Cell Dev. Biol.* **22** 713–719

Korecka JA, van Kesteren RE, Blaas E, Spitzer SO, Kamstra JH, Smit AB, Swaab DF, Verhaagen J and Bossers K 2013 Phenotypic characterization of retinoic acid differentiated SH-SY5Y cells by transcriptional profiling. *PLoS One* **8** e63862.

Kurki P, Ogata K and Tan EM 1988 Monoclonal antibodies to proliferating cell nuclear antigen (PCNA)/cyclin as probes for proliferating cells by immunofluorescence microscopy and flow cytometry. *J. Immunol. Methods* **109** 49–59

Kusakabe T, Motoki K and Hori K 1997 Mode of interactions of human aldolase isozymes with cytoskeletons. *Arch. Biochem. Biophys.* **344** 184–193

Lai WW, Yang JS, Lai KC, Kuo CL, Hsu CK, Wang CK, Chang CY, Lin JJ, Tang NY, Chen PY, Huang WW and Chung JG 2009 Rhein induced apoptosis through the endoplasmic reticulum stress, caspase- and mitochondria-dependent pathways in SCC-4 human tongue squamous cancer cells. *In Vivo* **23** 309–316

Lasorella A, Iavarone A and Israel MA 1995 Differentiation of neuroblastoma enhances Bcl-2 expression and induces alterations of apoptosis and drug resistance. *Cancer Res.* **55** 4711–4116

Lee Y-H, Liu X, Qiu F, O'Connor TR, Yen Y and Ann DK 2015 HP1β is a biomarker for breast cancer prognosis and PARP inhibitor therapy. *PLoS One* **10** e0121207

Legendre F, Heuze A, Boukerrouche K, Leclercq S, Boumediene K, Galera P, Domagala F, Pujol J-P and Ficheux H 2009 Rhein, the metabolite of diacerhein, reduces the proliferation of osteoarthritic chondrocytes and synoviocytes without inducing apoptosis. *Scand. J. Rheumatol.* **38** 104–411

Li Y, Wan OW, Xie W and Chung KKK 2011 P32 regulates mitochondrial morphology and dynamics through parkin. *Neuroscience* **199** 346–358

Li Q, Huang Y, Liu X, Gan J, Chen H and Yang C-G 2016 Rhein inhibits AlkB repair enzymes and sensitizes cells to methylated DNA damage. *J. Biol. Chem.* **291** 11083–11093

Licatalosi DD, Yano M, Fak JJ, Mele A, Grabinski SE, Zhang C and Darnell RB 2012 Ptbp2 represses adult-specific splicing to regulate the generation of neuronal precursors in the embryonic brain. *Genes Dev.* **26** 1626–1642

Lim J, Choi H-S and Choi HJ 2015 Estrogen-related receptor gamma regulates dopaminergic neuronal phenotype by activating GSK3β/NFAT signaling in SH-SY5Y cells. *J. Neurochem.* **133** 544–557

Liu Q, Zhang X-L, Tao R-Y, Niu Y-J, Chen X-G, Tian J-Y and Ye F 2011 Rhein, an inhibitor of adipocyte differentiation and adipogenesis. *J. Asian Nat. Prod. Res.* **13** 714–723

Liu N, Dai Q, Zheng G, He C, Parisien M and Pan T 2015 N6-methyladenosine-dependent RNA structural switches regulate RNA–protein interactions. *Nature* **518** 560–564

Lopes FM, Schröder R, da Frota ML Jr, Zanotto-Filho A, Müller CB, Pires AS, Meurer RT, Colpo GD, Gelain DP, Kapczinski F, Moreira JC, Fernandes Mda C and Klamt F 2010 Comparison between proliferative and neuron-like SH-SY5Y cells as an *in vitro* model for Parkinson disease studies. *Brain Res.* **1337** 85–94

Manakov D, Ujcikova H, Pravenec M and Novotny J 2016 The changes in the activity of some metabolic enzymes in the heart of SHR rat incurred by transgenic expression of CD36. *J. Proteomics* **145** 177–186

Mao Y, Zhang M, Yang J, Sun H, Wang D, Zhang X, Yu F and Li J 2017 The UCP2-related mitochondrial pathway participates in rhein-induced apoptosis in HK-2 cells. *Toxicol. Res.* **6** 297–304

Mattout A, Aaronson Y, Sailaja BS, Raghu Ram EV, Harikumar A, Mallm J-P, Sim KH, Nissim-Rafinia M, Supper E, Singh PB, Sze SK, Gasser SM, Rippe K and Meshorer E 2015 Heterochromatin protein 1β (HP1β) has distinct functions and distinct nuclear distribution in pluripotent versus differentiated cells. *Genome Biol.* **16** 213

McGee AM, Douglas DL, Liang Y, Hyder SM and Baines CP 2011 The mitochondrial protein C1qbp promotes cell proliferation, migration and resistance to cell death. *Cell Cycle* **10** 4119–4127

Neth B J and Craft S 2017 Insulin resistance and Alzheimer's disease: Bioenergetic linkages. *Front. Aging Neurosci.* **9** 345

Netto LES and Antunes F 2016 The roles of peroxiredoxin and thioredoxin in hydrogen peroxide sensing and in signal transduction. *Mol. Cells* **39** 65–71

Ojala JO, Sutinen EM, Salminen A and Pirttilä T 2008 Interleukin-18 increases expression of kinases involved in tau phosphorylation in SH-SY5Y neuroblastoma cells. *J. Neuroimmunol.* **205** 86–93

Paul S, Dansithong W, Kim D, Rossi J, Webster JG, Comai L and Reddy S 2006 Interaction of muscleblind, CUG-BP1 and hnRNP H proteins in DM1-associated aberrant IR splicing. *EMBO J.* **25** 4271–4283

Petersen-Mahrt SK, Estmer C, Öhrmalm C, Matthews DA, Russell WC and Akusjärvi G 1999 The splicing factor-associated protein, p32, regulates RNA splicing by inhibiting ASF/SF2 RNA binding and phosphorylation. *EMBO J.* **18** 1014–1024

Presgraves SP, Ahmed T, Borwege S and Joyce JN 2004 Terminally differentiated SH-SY5Y cells provide a model system for studying neuroprotective effects of dopamine agonists. *Neurotox. Res.* **5** 579–598

Ross RA, Spengler BA and Biedler JL 1983 Coordinate morphological and biochemical interconversion of human neuroblastoma cells. *J. Natl. Cancer Inst.* **71** 741–747

Shea TB, Perrone-Bizzozero NI, Beermann ML and Benowitz LI 1991 Phospholipid-mediated delivery of anti-GAP-43 antibodies into neuroblastoma cells prevents neuritogenesis. *J. Neurosci.* **11** 1685–1690

Sheng X, Wang M, Lu M, Xi B, Sheng H and Zang YQ 2011 Rhein ameliorates fatty liver disease through negative energy balance, hepatic lipogenic regulation, and immunomodulation in diet-induced obese mice. *AJP Endocrinol. Metab.* **300** E886–E893

Sinnamon JR, Waddell CB, Nik S, Chen EI and Czaplinski K 2012 Hnrpab regulates neural development and neuron cell survival after glutamate stimulation. *RNA* **18** 704–719

Sun Y-L, Cai J-Q, Liu F, Bi X-Y, Zhou L-P and Zhao X-H 2015 Aberrant expression of peroxiredoxin 1 and its clinical implications in liver cancer. *World J. Gastroenterol.* **21** 10840–10852

Sunabori T, Tokunaga A, Nagai T, Sawamoto K, Okabe M, Miyawaki A, Matsuzaki Y, Miyata T and Okano H 2008 Cell-cycle-specific nestin expression coordinates with morphological

changes in embryonic cortical neural progenitors. *J. Cell Sci.* **121** 1204–1212

Takano S, Wadhwa R, Yoshii Y, Nose T, Kaul S and Mitsui Y 1997 Elevated levels of mortalin expression in human brain tumors. *Exp. Cell Res.* **237** 38–45

Talukdar I, Sen S, Urbano R, Thompson J, Yates JR and Webster NJG 2011 hnRNP A1 and hnRNP F modulate the alternative splicing of exon 11 of the insulin receptor gene. *PLoS One* **6** e27869.

Tang N, Chang J, Lu H-C, Zhuang Z, Cheng H-L, Shi J-X and Rao J 2017 Rhein induces apoptosis and autophagy in human and rat glioma cells and mediates cell differentiation by ERK inhibition. *Microb. Pathog.* **113** 168–175

Ujcikova H, Eckhardt A, Kagan D, Roubalova L and Svoboda P 2014 Proteomic analysis of post-nuclear supernatant fraction and percoll-purified membranes prepared from brain cortex of rats exposed to increasing doses of morphine. *Proteome Sci.* **12** 11

Ujcikova H, Vosahlikova M, Roubalova L and Svoboda P 2016 Proteomic analysis of protein composition of rat forebrain cortex exposed to morphine for 10 days; comparison with animals exposed to morphine and subsequently nurtured for 20 days in the absence of this drug. *J. Proteomics* **145** 11–23

Walsh JL, Keith TJ and Knull HR 1989 Glycolytic enzyme interactions with tubulin and microtubules. *Biochim. Biophys. Acta* **999** 64–70

Wang CC 1998 Protein disulfide isomerase assists protein folding as both an isomerase and a chaperone. *Ann. N. Y. Acad. Sci.* **864** 9–13

Wong JC, Hasan MR, Rahman M, Yu AC, Chan SK, Schaeffer DF, Kennecke HF, Lim HJ, Owen D and Tai IT 2013 Nucleophosmin 1, upregulated in adenomas and cancers of the colon, inhibits p53-mediated cellular senescence. *Int. J. Cancer* **133** 1567–1577

Xie H, Hu L and Li G 2010 SH-SY5Y human neuroblastoma cell line: *In vitro* cell model of dopaminergic neurons in Parkinson's disease. *Chin. Med. J. (Engl).* **123** 1086–1092

Xu D-H, Liu F, Li X, Chen X-F, Jing G-J, Wu F-Y, Shi S-L and Li Q-F 2014 Regulatory role of nucleophosmin during the differentiation of human liver cancer cells. *Int. J. Oncol.* **45** 264–272

Xun Z, Lee D-Y, Lim J, Canaria CA, Barnebey A, Yanonne SM and McMurray CT 2012 Retinoic acid-induced differentiation increases the rate of oxygen consumption and enhances the spare respiratory capacity of mitochondria in SH-SY5Y cells. *Mech. Ageing Dev.* **133** 176–185

Yabe JT, Chan WK-H, Wang F-S, Pimenta A, Ortiz DD and Shea TB 2003 Regulation of the transition from vimentin to neurofilaments during neuronal differentiation. *Cell Motil. Cytoskelet.* **56** 193–205

Yan Y, Sabharwal P, Rao M and Sockanathan S 2009 The antioxidant enzyme Prdx1 controls neuronal differentiation by thiol-redox-dependent activation of GDE2. *Cell* **138** 1209–1221

Yang SY, He XY and Schulz H 1987 Fatty acid oxidation in rat brain is limited by the low activity of 3-ketoacyl-coenzyme A thiolase. *J. Biol. Chem.* **262** 13027–13032

Yoshikawa H, Komatsu W, Hayano T, Miura Y, Homma K, Izumikawa K, Ishikawa H, Miyazawa N, Tachikawa H, Yamauchi Y, Isobe T and Takahashi N 2011 Splicing factor 2-associated protein p32 participates in ribosome biogenesis by regulating the binding of Nop52 and fibrillarin to preribosome particles. *Mol. Cell. Proteomics* **10** M110.006148

Yu Y-M, Han P-L and Lee J-K 2003 JNK pathway is required for retinoic acid-induced neurite outgrowth of human neuroblastoma, SH-SY5Y. *NeuroReport* **14** 941–945

Zhang H, Chen L, Chen J, Jiang H and Shen X 2011 Structural basis for retinoic X receptor repression on the tetramer. *J. Biol. Chem.* **286** 24593–24598

Zhang Y, Fan S, Hu N, Gu M, Chu C, Li Y, Lu X and Huang C 2012 Rhein reduces fat weight in db/db mouse and prevents diet-induced obesity in C57Bl/6 mouse through the inhibition of PPAR γ signaling. *PPAR Res.* **2012** 1–9

Zhao X, Yang Y, Sun BF, Shi Y, Yang X, Xiao W, Hao YJ, Ping XL, Chen YS, Wang WJ, Jin KX, Wang X, Huang CM, Fu Y, Ge XM, Song SH, Jeong HS, Yanagisawa H, Niu Y, Jia GF, Wu W, Tong WM, Okamoto A, He C, Rendtlew Danielsen JM, Wang XJ and Yang YG 2014 FTO-dependent demethylation of N6-methyladenosine regulates mRNA splicing and is required for adipogenesis. *Cell Res.* **24** 1403–1419

Zheng J 2012 Energy metabolism of cancer: Glycolysis versus oxidative phosphorylation (review). *Oncol. Lett.* **4** 1151–1157

Zheng J-M, Zhu J-M, Li L-S and Liu Z-H 2008 Rhein reverses the diabetic phenotype of mesangial cells over-expressing the glucose transporter (GLUT1) by inhibiting the hexosamine pathway. *Br. J. Pharmacol.* **153** 1456–1464

Zhou Y-X, Xia W, Yue W, Peng C, Rahman K and Zhang H 2015 Rhein: A review of pharmacological activities. *Evid. Based Complement. Altern. Med.* **2015** 1–10

Corresponding editor: Aurnab Ghose